



NUMERICAL AND EXPERIMENTAL INVESTIGATION OF STEAM FILM CONDENSATION ON A VERTICAL TUBE

Wail S. Sarsam
Mech. Eng. Dept.
College of Engineering
University of Baghdad
Baghdad-Iraq

Luma F. Ali
Mech. Eng. Dept.
College of Engineering
University of Baghdad
Baghdad-Iraq

ABSTRACT

Film condensation of steam on a vertical tube is investigated numerically and experimentally, in the present work. A mathematical model was set based on the basic conservation laws of mass and energy, Nusselt's analysis of film condensation, and empirical equations available in the literature. Then, a simulation program in FORTRAN language was developed which simulates the film condensation of steam on a vertical tube. A complete steam tables subprogram was also developed and incorporated with the main program. The experimental work was carried out using a steam condensation test bench. The inlet and outlet cooling water temperatures, steam temperature and pressure, tube surface temperature at center, and cooling water flow rate are recorded during each experimental test run. The inlet cooling water temperature, steam temperature, and cooling water flow rate are used as an input for the numerical program, then the program calculates tube surface temperature distribution, cooling water temperature distribution, local heat transfer rate, local condensation heat transfer coefficient, condensate boundary layer thickness distribution, total heat transfer rate, and average condensation heat transfer coefficient. The effect of various parameters on the condensation heat transfer coefficient, such as steam temperature, steam-surface temperature difference, and the presence of non-condensable gas were investigated and reported graphically. It was found that increasing (steam-surface) temperature difference while keeping the steam temperature constant results in an increase in condensate boundary layer thickness, which in turn causes a decrease in condensation heat transfer coefficient. On the other hand, increasing steam temperature and keeping the (steam-surface) temperature difference constant leads to an increase in condensation heat transfer coefficient. In addition, the presence of non-condensable gas with different concentrations was also investigated and it was shown that it causes a noticeable reduction in the average condensation heat transfer coefficient. An equation for calculating average condensation heat transfer coefficient on a vertical tube was also developed. The experimental data obtained from the test runs were compared with numerical results and showed good agreement. Thus, it can be concluded that the present computational program is suitable for simulating steam condensation on a vertical tube.

الخلاصة

تمت دراسة تكثف بخار الماء الغشائي على انبوب عمودي، عددياً وعملياً، في البحث الحالي. تم وضع النموذج الرياضي بالاستناد الى قوانين الحفظ الأساسية للكتلة والطاقة وباستعمال معادلات تجريبية متوفرة في الأدبيات المنشورة. تم اعداد نموذج رياضي مستند على قوانين الحفظ الأساسية للكتلة والطاقة، تحليل نسلت للتكثف الغشائي، ومعادلات تجريبية متوفرة في الأدبيات المنشورة. ومن ثم اعداد برنامج محاكاة بلغة الفورتران لنمذجة تكثف بخار الماء الغشائي على إنبوب عمودي. كذلك تم بناء برنامج

فرعي لحساب خواص بخار الماء ودمجه مع البرنامج الرئيسي. العمل التجريبي نفذ باستعمال منصة إختبار تكثف بخار الماء. إن درجتي حرارة الدخول والخروج لماء التبريد، درجة حرارة وضغط بخار الماء، درجة حرارة الإنبوب السطحية في المركز، و نسبة تدفق ماء التبريد قد سجلت أثناء كل تشغيل إختباري عملي. لقد تم استخدام كل من درجة حرارة الدخول لماء التبريد، درجة حرارة بخار الماء، ونسبة تدفق ماء التبريد كمدخلات للبرنامج العددي، ثم يقوم البرنامج بحساب توزيع درجة حرارة سطح الإنبوب، توزيع درجة حرارة ماء التبريد، معدل انتقال الحرارة الموضعي، معامل انتقال الحرارة الموضعي بالتكثف، توزيع سمك طبقة السائل المتكثف المتاخمة، معدل انتقال الحرارة الكلي، ومعامل انتقال الحرارة المتوسط بالتكثف. تمت دراسة تأثير العوامل المختلفة على معامل انتقال الحرارة بالتكثف، مثل درجة حرارة البخار، الإختلاف بدرجة الحرارة بين بخار الماء و سطح الإنبوب، وكذلك وجود غاز غير قابل للتكثف. لقد وجد ان زيادة الإختلاف بدرجة الحرارة بين بخار الماء و سطح الإنبوب مع بقاء درجة حرارة البخار ثابتة يؤدي الى زيادة في سمك طبقة السائل المتكثف المتاخمة، والتي تسبب بدورها نقصان في معامل نقل الحرارة بالتكثف. من الناحية الأخرى، زيادة درجة حرارة بخار الماء وبقاء الإختلاف بدرجة الحرارة بين بخار الماء و سطح الإنبوب ثابتاً يؤدي إلى زيادة في معامل انتقال الحرارة بالتكثف. بالإضافة الى ذلك، تأثير وجود غاز غير قابل للتكثف بنسب مختلفة قد درس أيضاً ووجد بأنه يسبب تخفيض ملحوظ في معامل انتقال الحرارة بالتكثف. تم كذلك اعداد معادلة لحساب معامل انتقال الحرارة بالتكثف على انبوب عمودي. البيانات التجريبية التي تم الحصول عليها من التجارب العملية قورنت بنتائج البرنامج العددية وتم الحصول على توافق جيد بينهما. وبهذا، يمكن الاستنتاج بأن البرنامج الحسابي الحالي مناسب لنمذجة تكثف بخار الماء على إنبوب عمودي.

KEYWORDS: Film Condensation, Steam, Two-Phase, Vertical Tube, Non-Condensable.

INTRODUCTION

The problem of heat transfer with phase change received extensive attention in the literature due to its wide range of applications in such diverse fields as heat exchange systems, chemical processing plants, evaporative condensers, distillation facilities, chemical vapor deposition processes, and many other industrial applications, including nuclear power plants. One of these problems is the heat transfer analysis of film condensation which is an important area in the design of heat exchangers. This mode of heat transfer is often used because high heat transfer coefficients can be achieved. However, in practical operations of the condensers, small amounts of non-condensable gas may exist in working vapors due to characteristics of the system. It is well known that the presence of non-condensable gas in a vapor can greatly reduce the performance of the condensers (Collier, 1972).

The heat transfer rates of laminar film condensation on vertical or nearly vertical surfaces were first predicted by (Nusselt, 1916). In Nusselt analysis, the condensate film was assumed to be thin and to have negligible inertial effects. Furthermore, it was assumed that the shear stress at the liquid-vapor interface was zero and that the temperature profile within the condensate film was linear. Following the publication of Nusselt's findings, many researchers attempted to improve the accuracy of the original analysis by implementing more realistic assumptions. (Rohsenow, 1956) modified the Nusselt's analysis by including the energy convection in the heat balance equation, but neglecting the inertial effects and suggested the modified latent heat of evaporation to account for the effect of the condensate temperature profile.

The heat transfer characteristics for laminar filmwise condensation along a flat plate with variable surface temperature using Nusselt's theory were studied by (Hosokawa et al., 1999). They calculated the local and averaged heat transfer coefficients on a condensing surface temperature on the heat transfer characteristic and they found that this characteristic on a condensing surface depends on the temperature distribution on the surface. Furthermore, they also investigated the effects depending on whether the cooling water was flowing co- or counter-current to the direction of the condensate flow. Furthermore, (Moon et al., 1999) investigated the local heat transfer coefficient experimentally for the reflux condensation in a vertical tube in a countercurrent flow between the steam-air mixture and the condensate. It was concluded that the presence of the air in gas up flow causes a remarkable decrease of the heat transfer coefficients compared to the same flow rate of pure steam.



The effects of non-condensable gas on the direct contact film condensation of vapor mixture under an adiabatic wall condition were investigated by **(Lee et al., 2001)**. They carried out a series of experiments for condensation of the steam/air mixture into the water film on the nearly vertical wall. The air mass fraction, the velocity of the mixture, the water film flow rate, and the subcooling at the inlet were selected as the experimental parameters affecting the direct contact condensation heat transfer coefficients. They found that the average heat transfer coefficients decrease as the air-mass fraction of the mixture increase, due to air concentration resistance near the interface.

The effects of the flowing mixture of steam and air on the condensation heat transfer at atmospheric pressure varying the air concentration was accomplished experimentally by **(Chung et al., 2004)**. Rates of heat transfer had been measured on a single face of a water-cooled flat plate suspended vertically in a cylindrical test section as steam and mixtures of steam and air flowed over it. The test results for pure steam showed good agreement with the predictions of the Nusselt analysis of natural convection condensation and the steam flow didn't affect the heat transfer. Moreover, it was concluded that the small steam flow over the cooling plate showed negligible effect to the condensation heat transfer but the mixture flow enhanced the heat transfer substantially. Besides the same authors, **(Chung et al., 2004)** presented later experimental results comparing film-wise and drop-wise condensations of steam and mixtures of steam and air at atmospheric pressure. By using the same test rig, both film-wise and drop-wise condensation heat transfer rates were measured, varying the air concentration, on a single face of water-cooled flat plates suspended vertically in a cylindrical test section as steam and mixtures of steam and air flowed over it. In the pure steam cases, the drop-wise condensation showed much higher heat transfer rates than film-wise condensation, which showed good agreement with Nusselt theory of natural convection condensation. However, in the steam and air mixture cases, as expected, both modes of condensation fell in similar range of heat transfer rates and these rates of heat transfer were governed more by the thermal resistance of the air rich layer.

The accurate steady and unsteady numerical solutions of the full two-dimensional governing equations for the Nusselt problem were presented by **(Phan and Narain, 2007)**. The computational approach of the Nusselt problem, which is composed of film condensation of saturated vapor on a vertical wall, produced results in agreement with the Nusselt solution. In that work, it was shown that the waves and wave effects were quite sensitive to the presence or absence of the wall noise. This sensitivity to the frequency and wavelength spectrum of the wall noise was exploited either to suppress or enhance the wave effects. Also, the results for this problem affirmed that heat transfer rates and shear rates were significantly enhanced by the presence of waves. Afterward, **(Xu et al., 2008)** studied the laminar film condensation of saturated steam on an isothermal vertical plate. They reduced the two ordinary boundary layer equations of momentum and thermal energy to two ordinary differential equations by means of a set of similarity transformations. Their work showed the validity and the great potentially of the proposed technique for the nonlinear problems with multiple solutions.

A comprehensive investigation for the steady-state mixed convection of a condensate film on an isothermal vertical tube in dry saturated vapor with a forced flow was performed by **(Chang, 2008)**. His analysis took into account the inertia and convection effects in the condensate layer and the resistance at the liquid-vapor interface. The numerical results indicated that the effect of the forced-flow parameter increases as the thickness of the liquid condensate layer increases. Another related problem is that of **(Shang and Zhong, 2008)** applied successfully the dimensionless velocity component method to the laminar free film condensation from vapor-gas mixture for similarity analysis and transformation of whole system of the governing partial differential equations. The set of dimensionless variables of the transformed mathematical model greatly facilitates the analysis and calculation of the velocity, temperature and concentration fields, and heat and mass transfer of the film condensation from the vapor-gas mixture. It was confirmed that

the presence of the non-condensable gas is a device factor in decreasing the heat and mass transfer of the film condensation and it was found that an increase of the wall temperature will increase the negative effect of the non-condensable gas on heat and mass transfer of the film condensation from the vapor-gas mixture.

In order to investigate steam film condensation on a vertical tube, a mathematical model based on the basic conservation laws of mass and energy, Nusselt's analysis on film condensation, and empirical equations available in published literature is developed in the present work. Additionally, a computer program simulating steam film condensation on a vertical tube utilizing the above mathematical model is elaborated. Then, experimental test runs are carried out using a condensation unit test bench. The experimental data obtained are compared with the results of simulation program. The effects of various parameters on the condensation heat transfer coefficient, such as steam temperature, steam-surface temperature difference, and the presence of non-condensable gas are investigated and reported graphically.

MATHEMATICAL MODEL

The elemental volume taken into consideration is shown in **Fig. 1**. From which, it can be seen that cooling water moves upward through the inner diameter of the condenser tube from section $(x+ dx)$ to (x) , while the condensate film thickness increases in moving from section (x) to $(x+ dx)$. The liquid film starts forming at the top of the tube and flows downward under the influence of gravity. The thickness of the film increases in the flow direction (x) because of continued condensation at the liquid-vapor interface. Heat in the amount of (h_{fg}) is released during condensation and is transferred through the film to the tube surface at temperature (T_s) , which must be below the saturation temperature (T_{sat}) of the vapor for condensation to occur (**Cengel, 2003**).

The analytical relation for the heat transfer coefficient in film condensation on a vertical plate was first developed by (**Nusselt, 1916**) under the following simplifying assumptions:

- Both the plate and the vapor are maintained at constant temperatures of (T_{wall}) and (T_{sat}) , respectively, and the temperature across the liquid film varies linearly.
- Heat transfer across the liquid film is by pure conduction (no convection currents in the liquid film).
- The velocity of the vapor is low (or zero) so that it exerts no drag on the condensate (no viscous shear on the liquid-vapor interface).
- The flow of the condensate is laminar and the properties of the liquid are constant.
- The acceleration of the condensate layer is negligible.
- The volume element of condensate liquid film on a vertical plate considered in Nusselt's analysis is shown in **Fig. 2**, from which, a relation for calculating condensate liquid film thickness over a flat plate at any location (x) is given as;

$$\delta_x = \left[\frac{4 K_l \mu_l (T_s - T_{wall\ x}) x}{g \rho_l (\rho_l - \rho_v) h_{fg}} \right]^{1/4} \quad (1)$$

Also, the local value of condensation heat transfer coefficient $(h_{cond\ x})$ over a flat plate is given by;

$$h_{cond\ x} = \frac{K_l}{\delta_x} = \left[\frac{g \rho_l (\rho_l - \rho_v) h_{fg} K_l^3}{4 \mu_l (T_s - T_{wall\ x}) x} \right]^{1/4} \quad (2)$$

Then, the mean (average) value of condensation heat transfer coefficient over a flat plate and for the whole plate surface $(h_{cond\ av})$ is given by;



$$h_{cond\ av} = \frac{1}{L} \int_0^L h_{cond\ x} dx = 0.943 \left[\frac{g \rho_l (\rho_l - \rho_v) h_{fg} K_l^3}{\mu_l (T_s - T_{wall}) L} \right]^{1/4} \tag{3}$$

The condensate film in an actual condensation process is cooled further to some average temperature between (T_s) and $(T_{wall\ x})$, releasing more heat in the process. Therefore, the actual heat transfer will be larger. (Rohsenow, 1956) showed that the cooling of the liquid below the saturation temperature can be accounted for by replacing (h_{fg}) by the modified latent heat of vaporization (h'_{fg}) defined as;

$$h'_{fg} = h_{fg} + 0.68 C_{pl} (T_s - T_{wall\ x}) \tag{4}$$

For the calculation of the condensate film boundary layer thickness, Eq. (1) for steam condensation over a vertical plate derived by (Nusselt, 1916) was used, because the thickness of the condensate film boundary layer is small when compared with the tube diameter, and using the modified latent heat of vaporization (Rohsenow, 1956), Eq. (4). The buildup of the condensate liquid film starts from top of the tube while moving downward, while the cooling water comes from the bottom of the tube and moves upward. Thus, the numerical program was made to perform the simulation process starting from the top of the tube and moving downward with the condensate film boundary layer. Therefore, initial estimation of the outlet cooling water temperature must be made and an iteration process must be performed until reaching convergence for the inlet cooling water temperature through changing of the outlet cooling water temperature.

In Eq.(1), there exist two unknowns, the condensate film thickness (δ_x) and tube wall temperature $(T_{wall\ x})$, which requires estimation of the wall surface temperature and solving for condensate film thickness, then, heat transfer rate is calculated by two ways, first, by conduction from the liquid film surface at a temperature of (T_s) to an estimated outside tube surface at a temperature of $(T_{wall\ x})_{est}$, and second, by conduction and convection from an estimated outside tube surface at a temperature of $(T_{wall\ x})_{est}$ to the cooling water entering the element with a temperature of $(T_{w\ x})$, when both values of heat transfer rate become equal with a specified tolerance, then the estimated value of tube wall surface temperature is correct, otherwise, iteration process must be made by correcting the estimated tube wall surface temperature.

The heat transfer rate from the liquid film surface, which is assumed to be at steam temperature, through an elemental length(dx), shown in Fig. 1, with an outside surface temperature of $(T_{wall\ x})$ is equal to the heat transfer rate from the outside surface of the same element at a temperature of $(T_{wall\ x})$ to the cooling water entering the element with a temperature of $(T_{w\ x})$, this gives, (Incropera et al., 2007);

$$Q_x = \frac{T_s - T_{wall\ x}}{R_f} = \frac{T_{wall\ x} - T_{w\ x}}{R_t + R_{in}} \tag{5}$$

Where,

$$R_f = \frac{\ln((r_2 + \delta)/r_2)}{2 \pi K_l dx} \tag{6}$$

$$R_t = \frac{\ln(r_2/r_1)}{2 \pi K_t dx} \quad (7)$$

$$R_{in} = \frac{1}{h_{in} A_{x in}} \quad (8)$$

For the range of cooling water flow rates used, the Reynolds number values calculated showed that the flow is laminar. Also, for the length of tube used and range of Reynolds number values, it was found that the flow is neither hydro-dynamically nor thermally fully developed. Therefore, the correlation proposed by (Sieder and Tate, 1936) was used for the calculation of the inside convection heat transfer coefficient of the cooling water as;

$$Nu_{in} = \frac{h_{in} d_h}{K_l} = 1.86 \times \left[\text{Re Pr} \frac{d_h}{x} \right] \left[\frac{\mu}{\mu_{wall}} \right]^{0.14} \quad (9)$$

$$\text{Where, } \text{Re} = \frac{\rho_l V_l d_h}{\mu_l} \quad (10)$$

Eq. (9) is used with the following conditions; $\left[\begin{array}{l} \text{Hydrodynamic entry length} = 0.05 \text{ Re } d_h \\ \text{Thermal entry length} = 0.05 \text{ Re Pr } d_h \\ \text{Re} \leq 2300 \end{array} \right]$

The local condensation heat transfer coefficient ($h_{cond x}$) is calculated from the following relation;

$$h_{cond x} = \frac{Q_x}{(T_s - T_{wall x})(2 \pi dx r_2)} \quad (11)$$

While the average condensation heat transfer coefficient ($h_{cond av}$) can be calculated using the following relation;

$$h_{cond av} = \frac{Q_{tot}}{(T_s - T_{wall center})(2 \pi L r_2)} \quad (12)$$

STEAM TABLE FORMULATION

The steam table was developed as a subroutine for the simulation program. The steam and water properties were calculated using special correlation techniques including some numerical constants. Before calculating the steam and water thermodynamic properties, the following reduced dimensionless quantities were introduced as follows, (U K Steam Tables, 1970);

$$\beta = \frac{P_{sat}}{P_{cl}}, \text{ the reduced saturation pressure} \quad (13)$$

$$\theta = \frac{T}{T_{cl}}, \text{ the reduced temperature} \quad (14)$$



$$\chi = \frac{v}{v_{c1}}, \text{ the reduced volume} \tag{15}$$

$$\varepsilon = \frac{h}{P_{c1} v_{c1}}, \text{ the reduced enthalpy} \tag{16}$$

- Where, $P_{c1} = 221.2 \text{ bar}$ (exactly)
- $T_{c1} = 647.3^\circ \text{ K}$ (exactly)
- $v_{c1} = 0.00317 \text{ m}^3/\text{kg}$ (exactly)
- $P_{c1} v_{c1} = 70.1204 \text{ kJ/kg}$ (exactly)

The reduced saturation pressure (β) as a function of the reduced temperature (θ) was calculated using the following equation, (U K Steam Tables, 1970):

$$\beta = \exp \left[\frac{\frac{1}{\theta} \sum_{n=1}^5 K_n (1-\theta)^n}{1 + K_6(1-\theta) + K_7(1-\theta)^2} - \frac{+(1-\theta)}{+ K_8(1-\theta)^2 + K_9} \right] \tag{17}$$

All values of the numerical constants for the steam table correlations are available in tables listed in appendix (A). The steam table correlations were sub-divided into two groups as follows:

1. Correlations for Saturated Liquid Properties

a. Reduced Volume (χ)

$$\begin{aligned} \chi = & A_{11} a_5 Z^{-5/17} + \left[A_{12} + A_{13} \theta + A_{14} \theta^2 + A_{15} (a_6 - \theta)^{10} + A_{16} (a_7 + \theta^{19})^{-1} \right] \\ & - \left[(a_8 + \theta^{11})^{-1} (A_{17} + 2A_{18} \beta + 3A_{19} \beta^2) \right] \\ & - \left[A_{20} \theta^{18} (a_9 + \theta^2) \right] \left\{ -3(a_{10} + \beta)^{-4} + a_{11} \right\} \\ & + 3A_{21} (a_{12} - \theta) \beta^2 + 4A_{22} \theta^{-20} \beta^3 \end{aligned} \tag{18}$$

b. Reduced Enthalpy (ε)

$$\begin{aligned} \varepsilon = & A_0 \theta - \sum_{n=1}^{10} (n-2) A_n \theta^{n-2} + A_{11} \left[Z \left\{ 17 \left(\frac{Z}{29} - \frac{Y}{12} \right) + 50 \frac{Y'}{12} \right\} + a^4 \theta - (a^3 - 1) \theta Y Y' \right] Z^{-5/17} \\ & + \left\{ A_{12} - A_{14} \theta^2 + A_{15} (90 + a_6) (a_6 - \theta)^9 + A_{16} (20 \theta^{19} + a_7) (a_7 + \theta^{19})^{-2} \right\} \beta \\ & - (12 \theta^{11} + a_8) (a_8 + \theta^{11})^{-2} (A_{17} \beta + A_{18} \beta^2 + A_{19} \beta^3) \\ & + A_{20} \theta^{18} (17 a_9 + 19 \theta^2) \left\{ (a_{10} + \beta)^{-3} + a_{11} \beta \right\} + A_{21} a_{12} \beta^3 + 21 A_{22} \theta^{-20} \beta^4 \end{aligned} \tag{19}$$

Where,

$$Z = Y + (a_3 Y^2 - 2a_4 \theta + 2a_5 \beta)^{1/2} \quad (20)$$

$$Y = 1 - a_1 \theta^2 - a_2 \theta^{-6} \quad (21)$$

$$Y' = -2a_1 \theta + 6a_2 \theta^{-7} \quad (22)$$

c. Dynamic Viscosity (μ)

$$\mu = \mu_0 \times \exp \left[VR \times \sum_{i=0}^5 \sum_{j=0}^4 (BB_{i,j} (TR - 1)^i (VR - 1)^j) \right] \quad (23)$$

Where,

$$\mu_0 = \left\{ \left[\frac{1}{TR} \right]^{1/2} \left[\sum_{i=0}^3 AA_i TR^i \right]^{-1} \right\} \times 10^{-6} \quad (24)$$

$$TR = 647.27/T(K) \quad (25)$$

$$VR = 0.003147/\nu \quad (26)$$

d. Thermal Conductivity (K)

$$\begin{aligned} K \times 10^3 = & a_0 + a_1 \left[\frac{T}{T_0} \right] + a_2 \left[\frac{T}{T_0} \right]^2 + a_3 \left[\frac{T}{T_0} \right]^3 + a_4 \left[\frac{T}{T_0} \right]^4 \\ & + (P - P_{sat}) \left\{ b_0 + b_1 \left[\frac{T}{T_0} \right] + b_2 \left[\frac{T}{T_0} \right]^2 + b_3 \left[\frac{T}{T_0} \right]^3 \right\} \\ & + (P - P_{sat}) \left\{ c_0 + c_1 \left[\frac{T}{T_0} \right] + c_2 \left[\frac{T}{T_0} \right]^2 + c_3 \left[\frac{T}{T_0} \right]^3 \right\} \end{aligned} \quad (27)$$

2. Correlations for Saturated Vapor Properties

a. Reduced Volume (χ)

$$\chi = I_1 \theta / \beta - \sum_{r=1}^5 r \beta^{r-1} \sum_{s=1}^{n(r)} B_{rs} X^{z(r,s)} + 11 \left(\frac{\beta}{\beta_L} \right)^{10} \sum_{s=0}^6 \beta_{9s} X^s - \sum_{r=6}^8 \frac{(r-2) \beta^{1-r} \sum_{s=1}^{n(r)} B_{rs} X^{z(r,s)}}{\left\{ \beta^{z-r} + \sum_{d=1}^{l(r)} b_{rd} X^{x(r,d)} \right\}^2} \quad (28)$$

b. Reduced Enthalpy (ϵ)

$$\begin{aligned}
 \varepsilon = & B_0\theta - \sum_{s=0}^5 B_{0s}(s-2)\theta^{s-1} - \sum_{r=1}^5 \beta^r \sum_{s=1}^{n(r)} B_{rs}(1+Z(r,s)b\theta)X^{Z(r,s)} \\
 & - \sum_{r=6}^8 \frac{\sum_{s=1}^{n(r)} B_{rs} X^{Z(r,s)} \left\{ (1+Z(r,s)b\theta) - \frac{b\theta \sum_{d=1}^{l(r)} X(r,d)b_{rd} X^{x(r,d)}}{\beta^{2-r} + \sum_{d=1}^{l(r)} b_{rd} X^{x(r,d)}} \right\}}{\beta^{2-r} + \sum_{d=1}^{l(r)} b_{rd} X^{x(r,d)}} \\
 & + \beta \left(\frac{\beta}{\beta_L} \right)^{10} \sum_{s=0}^6 \left[\left\{ 1 + \left(\frac{10\beta'_L}{\beta_L} + sb \right) \right\} B_{9s} X^s \right]
 \end{aligned} \tag{29}$$

Where,

$$X = \exp \{b(1 - \theta)\} \tag{30}$$

$$\beta_L = L_0 + L_1\theta + L_2\theta^2 \tag{31}$$

$$\beta'_L = \frac{d\beta_L}{d\theta} = L_1 + 2L_2\theta \tag{32}$$

COMPUTER PROGRAM FLOW CHART

The mathematical model described previously was solved numerically through a numerical calculation algorithm implemented by a developed computer program written in FORTRAN language. The flow chart of the computer program is shown in **Fig. (3)**. The inlet cooling water temperature, steam temperature, and cooling water flow rate are used as an input for the numerical program, then the program calculates tube surface temperature distribution, cooling water temperature distribution, local heat transfer rate, local condensation heat transfer coefficient, condensate boundary layer thickness distribution, total heat transfer rate, and average condensation heat transfer coefficient.

EXPERIMENTAL TEST RIG

A bench-top condensation unit manufactured by Gunt, which is a German company, is used for performing the experimental work. It consists of the following parts, (see **Fig. 4**);

(**1.** Socket for PC interface, **2.** Display and control panel, **3.** Vessel (Glass cylinder), **4.** Electric heater with power adjuster, **5.** Cooling water connections, **6.** Water jet vacuum pump, **7.** Water jet vacuum pump adjustment valve, **8.** Flow rate sensor, **9.** Temperature sensor, **10.** Cooling water adjustment valve, **11.** Condenser tubes, **12.** Pressure switch, **13.** Condensate separator, **14.** Drop collector, and **15.** Level sensor).

The bench-top unit provides clear demonstrations of condensation processes in a glass cylinder. The system has one condensation tube with a polished gold-plated surface for drop-wise condensation, and one condensation tube with a matt surface for film-wise condensation, which is investigated in the present work. The two condenser tubes are fitted in the upper part of the vessel. Cooling water flows upward through the inside of the condenser tubes. The heat given off by the steam at the condensation tubes can be determined from the measurement of the feed (inlet) and return (outlet) temperatures and the mass flow rate of the cooling water. The inlet and outlet water temperatures are measured via a PTC sensor with transmitter. The flow rate of cooling water is adjusted via control valves. The electric heater is in the lower part of the vessel, the output power of

the heater is adjustable. The temperature of the steam is measured using a PTC sensor mounted in the upper part of the vessel. While the tube surface temperature is measured via a type (J) thermocouple fixed on the outside surface of each tube in the middle.

The vessel is equipped with a pressure sensor to measure steam absolute pressure and a pressure switch to switch off the heater in the event of excessive overpressure. The vessel can be evacuated using a water jet vacuum pump. In order to prevent the escape of steam from the vessel, the suction pipe of the vacuum pump is fitted with cooling system and a water separator. The inlet and outlet cooling water temperatures, steam temperature and pressure, tube surface temperature at center, and cooling water flow rate are all recorded during each experimental test run. All parameters are measured electronically and displayed digitally.

RESULTS AND DISCUSSION

The effect of various parameters on the condensation heat transfer coefficient, steam pressure, steam-surface temperature difference and the presence of non-condensable gas, were investigated both experimentally and numerically and then reported graphically. In addition, the numerical results of the simulation program were compared with the data recorded in the experimental work in order to validate the numerical simulation program.

Figs. 5 to 7 show the predicted values of tube surface temperature at center, outlet cooling water temperature and average condensation heat transfer coefficient, respectively, versus corresponding experimental data recorded during test runs for different values of steam temperature and (steam-surface) temperature difference. **Fig. 5** shows good agreement between the numerical and predicted values. While **Fig. 6** shows that the experimental outlet cooling water temperature is always higher than the predicted one, and that the difference between them increases with increasing steam temperature. This behavior may be attributed to the fact that the heat transfer to the cooling water continues even after the water leaves the effective length of condenser tube until it reaches the point where the outlet cooling water thermocouple is fixed. This makes the thermocouple reading always higher than the predicted value with noticeable error. This relatively large error in the outlet cooling water temperature leads to a relatively large difference between the predicted and experimental values of the average condensation heat transfer coefficient shown in **Fig. 7**, which shows a maximum error of about (23 %). From the above three figures, it can be concluded that the numerical program can be used to simulate the condensation of steam on a vertical tube with acceptable accuracy.

The variation of predicted tube surface temperature along the condenser tube for different values of steam temperature and for a (steam-surface) temperature difference of (6.5 °C) is shown in **Fig. 8**. From which, it is clear that higher steam temperature leads, as expected, to a higher tube surface temperature. Also, it can be noticed that the decrease of surface temperature is approximately linear until reaching a point near the end of tube where the drop in temperature becomes faster, which may explained by the fact that the cooling water enters the condenser tube at the bottom and flows upward, and since the convection heat transfer coefficient at the tube entry is maximum, then the heat transfer rate to the cooling water will be higher and this will cause a faster reduction in tube surface temperature.

The cooling water temperature distribution curves along the condenser tube at different values of steam temperature and for an inlet water temperature of (20.1 °C) and a water flow rate of (30 l/h) are shown in **Fig. 9**. From which, it is clear that higher steam temperature gives a higher cooling water temperature along the entire tube length, which results from a higher tube surface temperature at high steam temperature shown in **Fig. 8**.

The local heat transfer rate (Q_x) distribution curves along the condenser tube at different values of (steam-surface) temperature difference and for a steam temperature of (95 °C) are shown in **Fig. 10**. From which, it is obvious that increasing (steam-surface) temperature difference increases the local heat transfer rate along the whole tube. Also, it can be observed that local heat

transfer rate increases relatively slow at the beginning of the tube, then speed up a little towards the tube end, which may explained by the fact the cooling water have a maximum convection heat transfer coefficient at its entry to the condenser tube at the bottom.

The distribution curves of local heat transfer rate (Q_x) along the condenser tube at different values of steam temperature and for a (steam-surface) temperature difference of (6.5 °C) are shown in **Fig. 11**. From which, it is apparent that increasing steam temperature increases the local heat transfer rate along the entire tube length. Also, it can be observed that local heat transfer rate increases relatively slow at the beginning of the tube, then speed up a little towards the tube end. This trend may be explained in the same way as that of **Fig. 10**.

Curves representing a plot of condensate film thickness along the condenser tube at different values of (steam-surface) temperature difference and for a steam temperature of (95 °C) are shown in **Fig. 12**. From which, it is clear that higher condensate boundary layer thickness is obtained at higher values of (steam-surface) temperature difference, which is understandable from observing that the higher local heat transfer rates (Q_x) occur at higher values of (steam-surface) temperature difference shown in **Fig. 10**.

The local values of condensation heat transfer coefficient distribution curves along the condenser tube at different values of (steam-surface) temperature difference and for a steam temperature of (95 °C) are shown in **Fig. 13**. From which, it is obvious that the local condensation heat transfer coefficient increases with decreasing (steam-surface) temperature difference, since decreasing (steam-surface) temperature difference causes a decrease in the condensate boundary layer which is clearly shown in **Fig. 12**. The growth in condensate film thickness represents an increase in conductive resistance of the film and thus reducing local value of condensation heat transfer coefficient. In addition, the local value of condensation heat transfer coefficient decreases while moving towards the tube end because of the increase of condensate boundary layer thickness.

Curves representing the distribution of local values of condensation heat transfer coefficient along the condenser tube at different values of steam temperature and for a (steam-surface) temperature difference of (6.5 °C) are shown in **Fig. 14**. From which, it is noticeable that the local condensation heat transfer coefficient increases with increasing steam temperature.

The experimentally calculated values of average condensation heat transfer coefficient are plotted versus their corresponding steam temperatures in **Fig. 15** for two cases, pure steam and with presence of non-condensable gas (air) at different concentrations. From which, it can proved that the presence of non-condensable gas with the pure steam even with small concentration can cause a remarkable reduction in the condensation heat transfer coefficient and heat transfer rate, which is a fact observed by many experimental researches in this field. The non-condensable gas can cause a drop in the condensation heat transfer coefficient even to a value of about (10 %) of that for pure steam.

Points representing the intersection of the experimentally calculated values of average condensation heat transfer coefficient with numerical values of the right hand side of Eq. 3 defined as, $\left[\frac{g \rho_l (\rho_l - \rho_v) h_{fg} K_l^3}{\mu_l (T_s - T_{wall}) L} \right]^{1/4}$, are shown in **Fig. 16**. Through these points, a line which best fits them is drawn, and it is found that a factor of (1.087) gives the slope of this line, therefore, it can be concluded that an equation for calculating average condensation heat transfer coefficient on a vertical tube can be written as;

$$h_{cond\ av} = 1.087 \left[\frac{g \rho_l (\rho_l - \rho_v) h_{fg} K_l^3}{\mu_l (T_s - T_{wall}) L} \right]^{1/4} \quad (33)$$

CONCLUSIONS

It was concluded that the values of tube surface temperature and cooling water temperature increase with increasing steam temperature for the same value of (steam-surface) temperature difference. From the elemental heat transfer rate distribution curves, it can be deduced that the heat transfer rate increases with increasing steam temperature and keeping the (steam-surface) temperature difference constant or with increasing (steam-surface) temperature difference and maintaining the steam temperature constant. It was found that increasing (steam-surface) temperature difference while keeping the steam temperature constant results in an increase in condensate boundary thickness, which in turn causes a decrease in condensation heat transfer coefficient. On the other hand, increasing steam temperature and keeping the (steam-surface) temperature difference constant leads to an increase in condensation heat transfer coefficient. In addition, the presence of non-condensable gas with different concentrations was also investigated and it was shown that it causes a noticeable reduction in the average condensation heat transfer coefficient even to a value of about (10 %) of that with pure steam. An equation for calculating average condensation heat transfer coefficient on a vertical was developed, which is given by Eq. 33.

REFERENCES

- Cengel, Y. A., (2003), "Heat transfer - A Practical Approach", 2nd edition, McGraw-Hill Book Company. (Internet Search)
- Chung B., Kim S., and Kim M. C., (2004), "An Experimental Investigation of Film Condensation of Flowing Mixtures of Steam and Air on a Vertical Flat Plate", Int. Comm. Heat Mass Transfer, Vol. 31, pp. 703-710.
- Chung B., Kim S., and Kim M. C., (2004), "Experimental Comparison of Film-Wise and Drop-Wise Condensations of Steam on a Vertical Flat Plates with the Presence of Air", Int. Comm. Heat Mass Transfer, Vol. 31, pp. 1067-1074.
- Chang T., (2008), "Mixed Convection Film Condensation along Outside Surface of Vertical Tube in Saturated Vapor with Forced Flow", Appl. Therm. Eng., Vol. 28, pp. 547-555.
- Collier J. G., (1972), "Convective Boiling and Condensation", McGraw-Hill Book Company, New York.
- Hosokawa T., Entesari-Tatafi J., Kawashima Y., and Kimura F., (1999), "Heat Transfer Characteristics for Laminar Filmwise Condensation Along a Flat Vertical Plate with Three Distinct Cooling Zones", Second Int. Conf. on CFD in the Minerals and Process Industries CSIRO, Melbourne, Australia, 6-8 Dec.
- Incropera, DeWitt, Bergman, and Lavine, (2007), "Fundamentals of Heat and Mass Transfer", 6th edition, Wiley Book Company. (Internet Search)
- Lee H., Kim M., and Park S., (2001), "The Effect of Non-Condensable Gas on Direct Contact Condensation of Steam/Air Mixture", J. Korean Nuclear Society, Vol. 33, pp. 585-595.



- Moon Y. M., No H. C., and Bang Y. S., (1999), "Local Heat Transfer Coefficients for Reflux Condensation Experiment in a Vertical Tube in the Presence of Non-Condensable Gas", J. Korean Nuclear Society, Vol. 31, pp. 486-497.
- Nusselt W., (1916), "Die oberflächen Kondensation des Wasserdampfes", Z. Ver. Deut. Ing., Vol. 60, (2) pp. 541-546. (cited in (Collier, 1972))
- Phan L., and Narain A., (2007), "Nonlinear Stability of the Classical Nusselt Problem of Film Condensation and Wave Effects ", ASME, J. Appl. Mech., Vol. 74.
- Rohsenow W. M., (1956), "Heat Transfer and Temperature Distribution in Laminar-Film Condensation", Trans. ASME, J. Heat Transfer, Vol. 78, pp. 1645-1648. (cited in (Collier, 1972))
- Shang D., and Zhong L., (2008), "Extensive Study on Laminar Free Film Condensation from Vapor-Gas Mixture", Int. J. Heat Mass Transfer, Vol. 51.
- Sieder E. N., and Tate G. E., (1936), "Heat transfer and Pressure Drop of Liquids in Tubes", Ind. Eng. Chem., Vol. 28, pp. 1429-1435.
- Xu H., You X., and Pop I., (2008), "Analytical Approximation for Laminar Film Condensation of Saturated Steam on an Isothermal Vertical Plate", Appl. Math. Modeling, Vol. 32, pp. 738-748.

NOMENCLATURE

Latin Symbols

A = surface area [m²].
b = width [m].
C_p = specific heat at constant pressure [J/kg °C].
d = diameter of tube [m].
d_h = hydraulic diameter [m].
dx = length of element [m].
g = acceleration of gravity [m/s²].
h = enthalpy [J/kg].
h_{cond} = condensation H.T.C. [W/m².°C].
h_{in} = forced convection H.T.C. [W/m².°C].
h_{fg} = latent heat of vaporization [J/kg].
K = thermal conductivity [W/m.°C].
L = tube length [m].
 \dot{m} = mass flow rate [kg/s].
Nu = Nusselt number, dimensionless.
P = pressure [N/m²].
Pr = Prandtl number, dimensionless.
Q = heat transfer rate [W].
R = thermal resistance [°C/W].
Re = Reynolds number, dimensionless.
r₁ = inner tube diameter [m].
r₂ = outer tube diameter [m].

u = velocity [m/s].

V = cooling water velocity [m/s].

x = tube axial length (vertical-coordinate) [m].

y = y-axis (horizontal-coordinate) [m].

Greek Symbols

δ = condensate boundary layer thickness [m].

μ = dynamic viscosity [kg/s.m].

v = specific volume = 1/ρ [m³/kg].

ρ = density [kg/m³].

Subscripts

av = average.

est = estimated.

f = liquid film.

in = inside, inlet.

l = liquid.

out = outlet

s = steam.

sat = saturation.

t = tube.

tot = total.

v = vapor.

w = water.

wall = tube surface.

T = temperature [$^{\circ}\text{C}$ or K].

x = local value at any (x).

APPENDIX (A)

Numerical Constants for the Steam Table Correlations (U K Steam Tables, 1970).

Table 1 Values of numerical constants for Eq. (17)

$K_1 = -7.691234564 \times 10^0$	$k_2 = -2.608023696 \times 10^1$	$k_3 = -1.681706546 \times 10^2$	$k_4 = 6.423285504 \times 10^1$
$k_5 = -1.189646225 \times 10^2$	$k_6 = 4.167117320 \times 10^0$	$k_7 = 2.097506760 \times 10^1$	$k_8 = 10^9$ $k_9 = 6$

Table 2 Values of numerical constants for Eqs. (18) to (22)

$A_0 = 6.824687741 \times 10^3$	$A_1 = -5.422063673 \times 10^2$	$A_2 = -2.096666205 \times 10^4$	$A_3 = 3.941286787 \times 10^4$
$A_4 = -6.733277739 \times 10^4$	$A_5 = 9.902381028 \times 10^4$	$A_6 = -1.093911774 \times 10^5$	$A_7 = 8.590841667 \times 10^4$
$A_8 = -4.511168742 \times 10^4$	$A_9 = 1.418138926 \times 10^4$	$A_{10} = -2.01727113 \times 10^3$	$A_{11} = 7.982692717 \times 10$
$A_{12} = -2.616571843 \times 10^{-2}$	$A_{13} = 1.52241179 \times 10^{-3}$	$A_{14} = 2.2842279054 \times 10^{-2}$	$A_{15} = 2.421647003 \times 10^2$
$A_{16} = 1.269716088 \times 10^{-10}$	$A_{17} = 2.074838328 \times 10^{-7}$	$A_{18} = 2.17402035 \times 10^{-8}$	$A_{19} = 1.105710498 \times 10^{-9}$
$A_{20} = 1.293441934 \times 10$	$A_{21} = 1.308119072 \times 10^{-5}$	$A_{22} = 6.047626338 \times 10^{-14}$	$a_1 = 8.438375405 \times 10^{-1}$
$a_2 = 5.362162162 \times 10^{-4}$	$a_3 = 1.72 \times 10$	$a_4 = 7.342278489 \times 10^{-2}$	$a_5 = 4.97585887 \times 10^{-2}$
$a_6 = 6.5371543 \times 10$	$a_7 = 1.15 \times 10^{-6}$	$a_8 = 1.5108 \times 10^{-5}$	$a_9 = 1.4188 \times 10^{-1}$
$a_{10} = 7.002753165 \times 10$	$a_{11} = 2.995284926 \times 10^{-4}$	$a_{12} = 2.04 \times 10^{-1}$	

Table 3 Values of numerical constants for Eqs. (23) and (24)

$AA_0 = 0.0181583, AA_1 = 0.0177624, AA_2 = 0.0105287, AA_3 = -0.0036744$					
$BB_{i,j}$					
	$j = 0$	1	2	3	4
$i = 0$	0.501938	0.235622	-0.274637	0.145831	-0.0270448
1	0.162888	0.789393	-0.743539	0.263129	-0.0253093
2	-0.130356	0.673665	-0.959456	0.347247	-0.0267758
3	0.907919	1.207552	-0.687343	0.213486	-0.0822904
4	-0.551119	0.0670665	-0.497089	0.100754	0.0602253
5	0.146543	-0.084337	0.195286	-0.032932	-0.0202595

Table 4 Values of numerical constants for Eq. (27)

$a_0 = -922.47$	$a_1 = 2839.5$	$a_2 = -1800.7$	$a_3 = 525.77$	$a_4 = -73.44$
$b_0 = -0.9473$	$b_1 = 2.5186$	$b_2 = -2.0012$	$b_3 = 0.5186$	$c_0 = 1.6563 \times 10^{-3}$
$c_1 = -3.8929 \times 10^{-3}$	$c_2 = 2.9323 \times 10^{-3}$	$c_3 = -7.1693 \times 10^{-4}$	$T_0 = 273.15^{\circ}\text{K}$	

Table 5 Values of numerical constants for Eqs. (28) to (32)

$I_1 = 4.260321148 \times 10$	$L_0 = 1.574373327 \times 10^1$	$L_1 = -3.417061978 \times 10^1$	$L_2 = 1.931380707 \times 10^1$
$B_0 = 1.683599274 \times 10^1$	$B_{01} = 2.856067796 \times 10^1$	$B_{02} = -5.438923329 \times 10^1$	$B_{03} = 4.330662834 \times 10^{-1}$
$B_{04} = -6.547711697 \times 10^{-1}$	$B_{05} = 8.565182058 \times 10^{-2}$	$B_{11} = 6.670375918 \times 10^{-2}$	$B_{12} = 1.388983801 \times 10$
$B_{21} = 8.390104328 \times 10^{-2}$	$B_{22} = 2.614670893 \times 10^{-2}$	$B_{23} = -3.373439453 \times 10^{-2}$	$B_{31} = 4.520918904 \times 10^{-1}$
$B_{32} = 1.069036614 \times 10^{-1}$	$B_{41} = -5.975336707 \times 10^{-1}$	$B_{42} = -8.847535804 \times 10^{-2}$	$B_{51} = 5.958051609 \times 10^{-1}$
$B_{52} = -5.159303373 \times 10^{-1}$	$B_{53} = 2.075021122 \times 10^{-1}$	$B_{61} = 1.190610271 \times 10^{-1}$	$B_{62} = -9.867174132 \times 10^{-2}$



$B_{71} = 1.683998803 \times 10^{-1}$	$B_{72} = -5.809438001 \times 10^{-2}$	$B_{81} = 6.552390126 \times 10^{-3}$	$B_{82} = 5.710218648 \times 10^{-4}$
$B_{90} = 1.936587558 \times 10^2$	$B_{91} = -1.388522425 \times 10^3$	$B_{92} = 4.126607219 \times 10^3$	$B_{93} = -6.508211677 \times 10^3$
$B_{94} = 5.745984054 \times 10^3$	$B_{95} = -2.693088365 \times 10^3$	$B_{96} = 5.235718623 \times 10^2$	$b = 7.633333333 \times 10^{-1}$
$b_{61} = 4.006073948 \times 10^{-1}$	$b_{71} = 8.636081627 \times 10^{-2}$	$b_{81} = -8.532322921 \times 10^{-1}$	$b_{82} = 3.460208861 \times 10^{-1}$

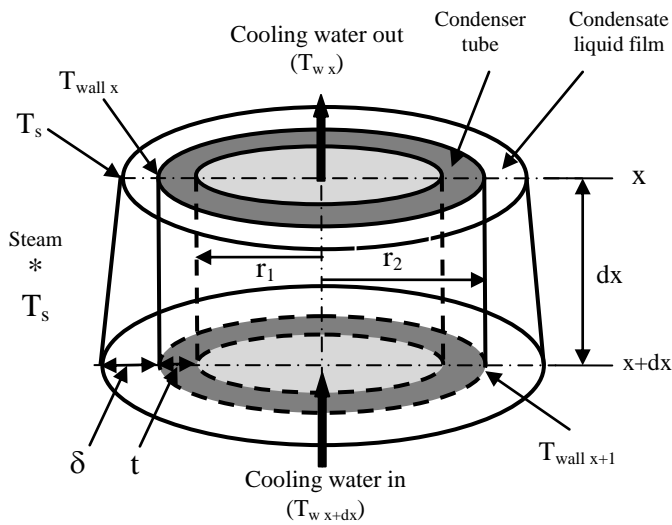


Fig. (1) The elemental volume considered in the present work.

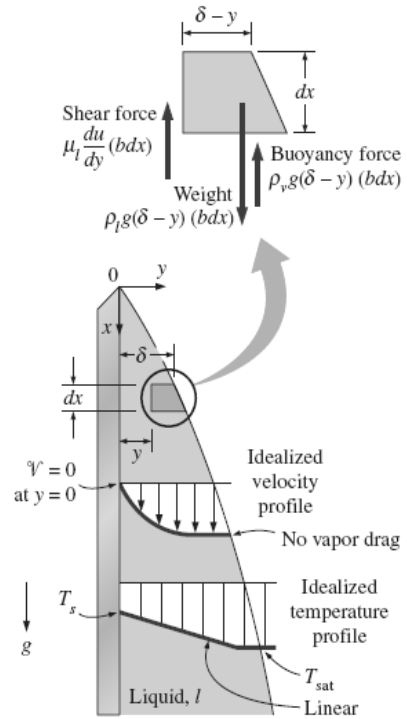


Fig. (2) The volume element of condensate on a vertical plate considered in Nusselt's analysis. (Cengel, 2003)

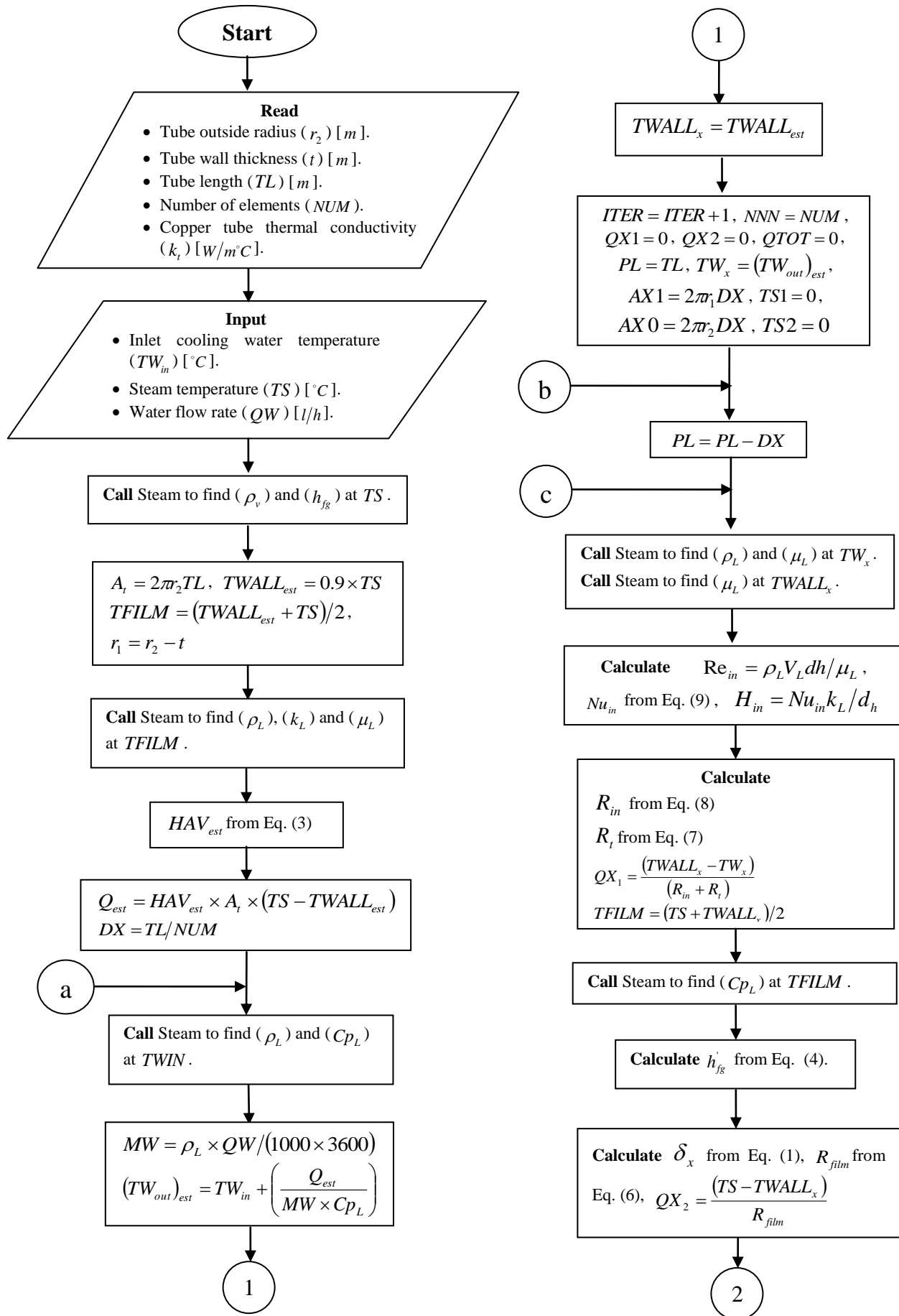


Fig. (3) Computer Program Flow Chart.

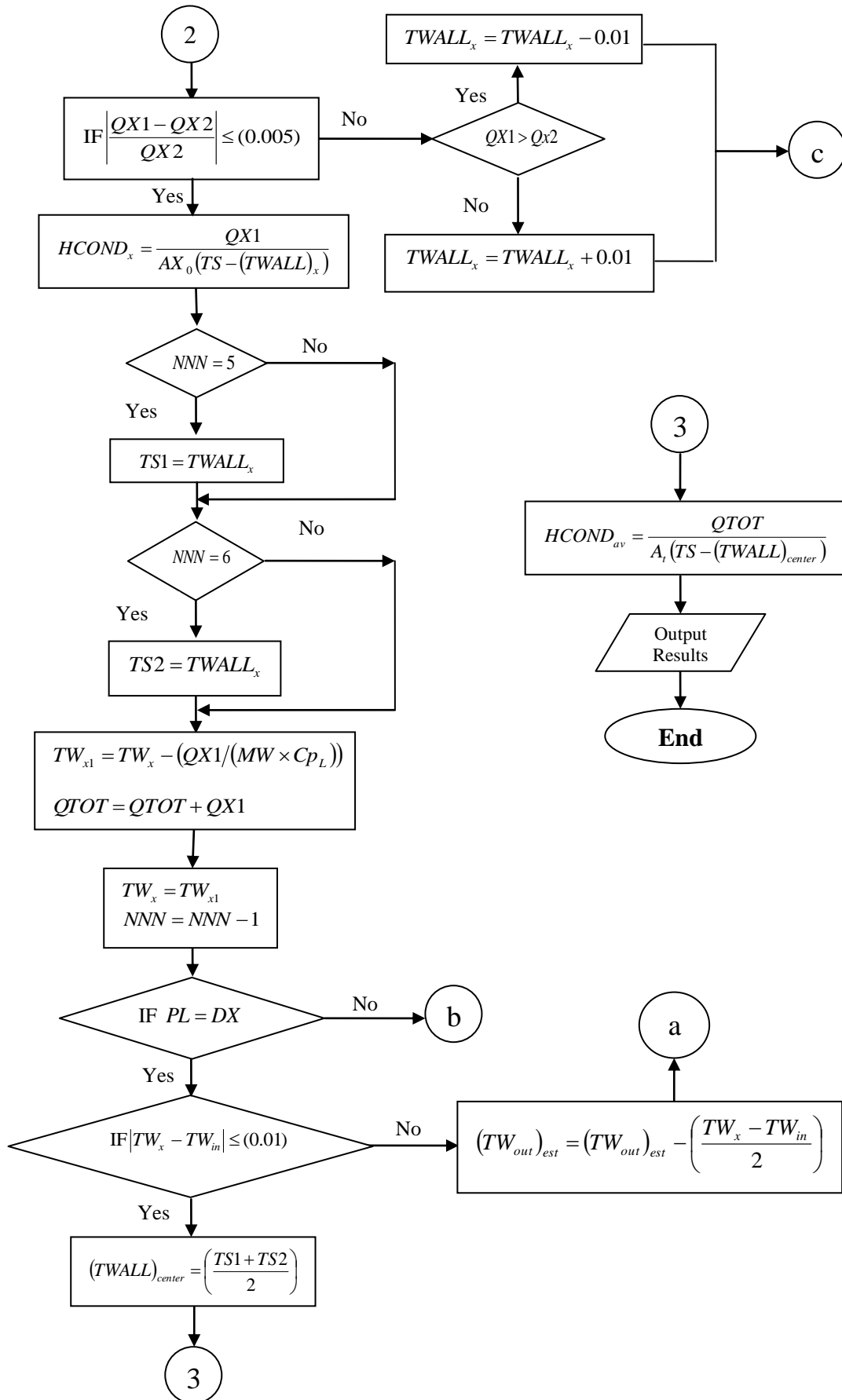


Fig. (3) Continued.

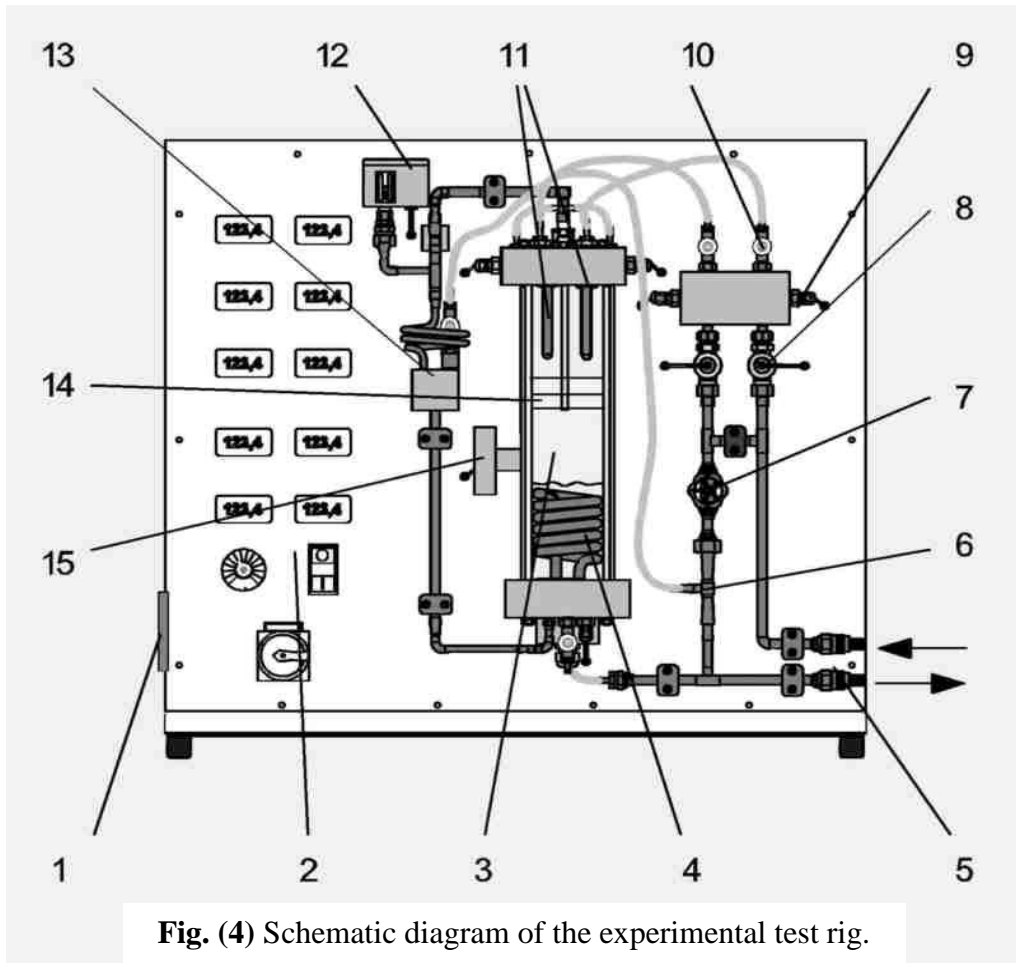


Fig. (4) Schematic diagram of the experimental test rig.

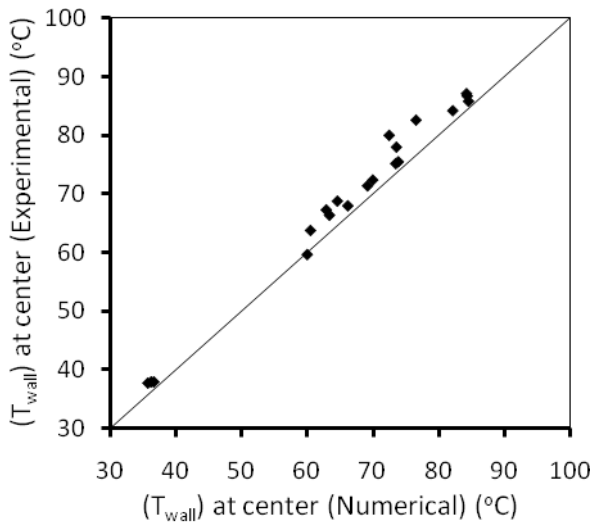


Fig. (5) Predicted tube surface temperature at center versus experimental data.

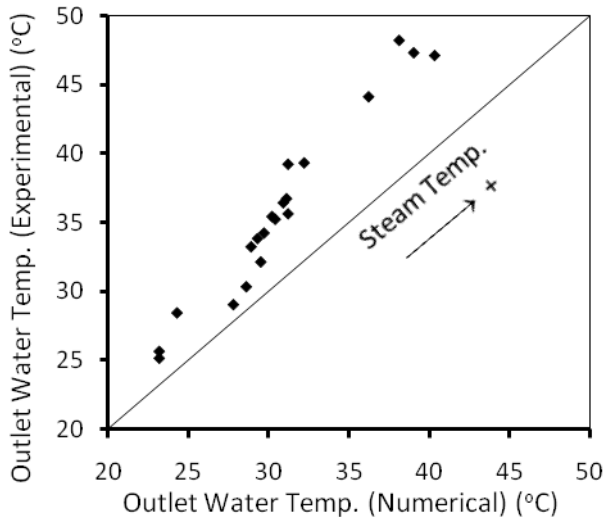


Fig. (6) Predicted cooling water outlet temperature versus experimental data.

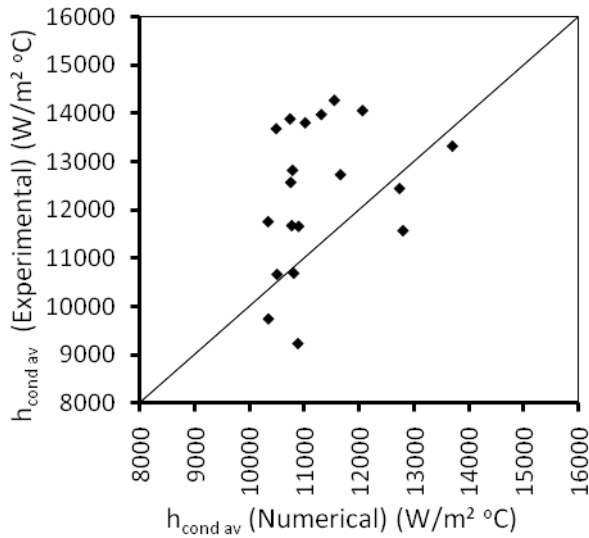


Fig. (7) Predicted condensation heat transfer coefficient versus experimental data.

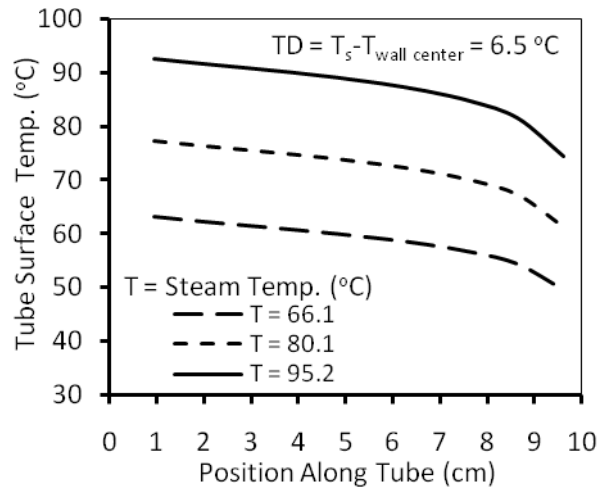


Fig. (8) Variation of tube surface temperature with position along tube for different (steam-surface) Temp. difference.

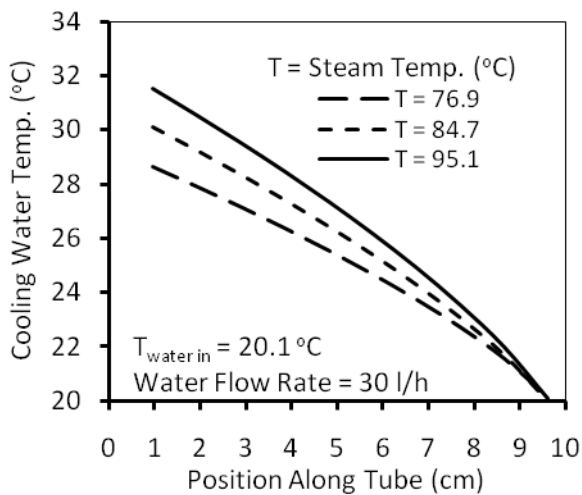


Fig. (9) Distribution of cooling water temperature flowing through the tube for different steam temperatures.

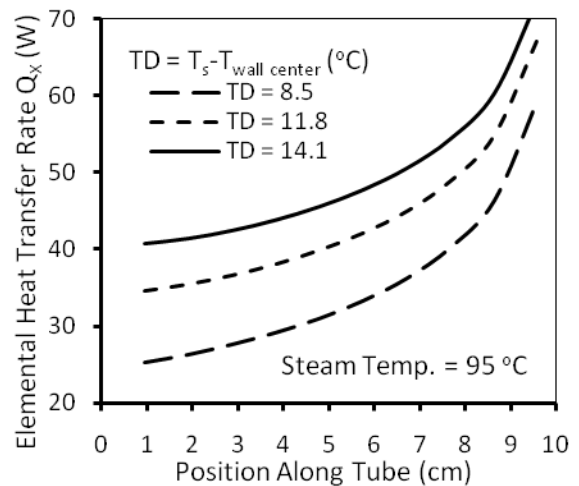


Fig. (10) Variation of local heat transfer rate with position along tube for different (steam-surface) Temp. difference.

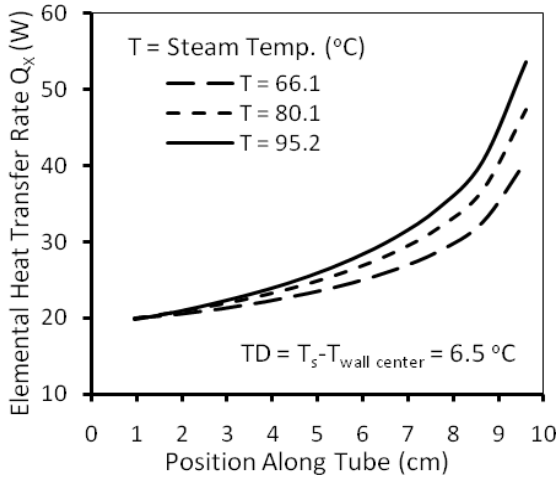


Fig. (11) Variation of local heat transfer rate with position along tube for different steam temperatures.

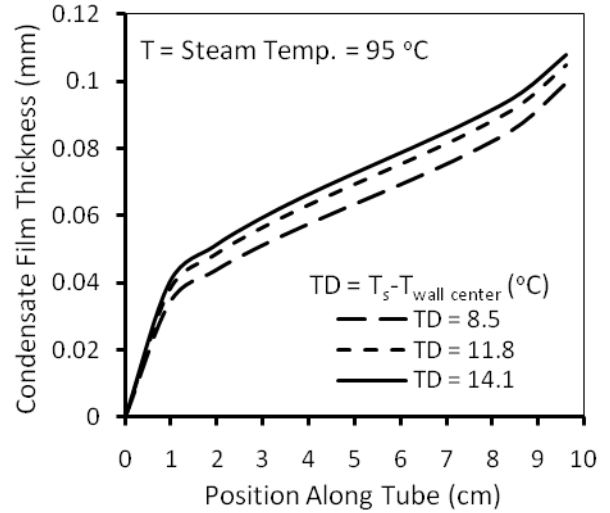


Fig. (12) Distribution of condensate film thickness along tube surface for different steam temperatures.

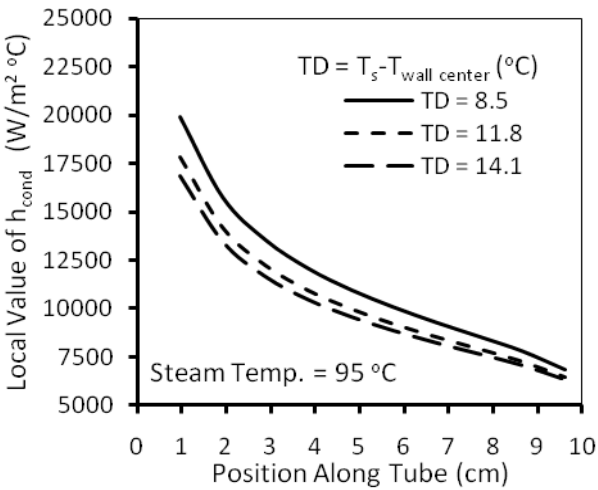


Fig. (13) Variation of local condensation H.T. coefficient with position along tube for different (steam-surface) Temp. difference.

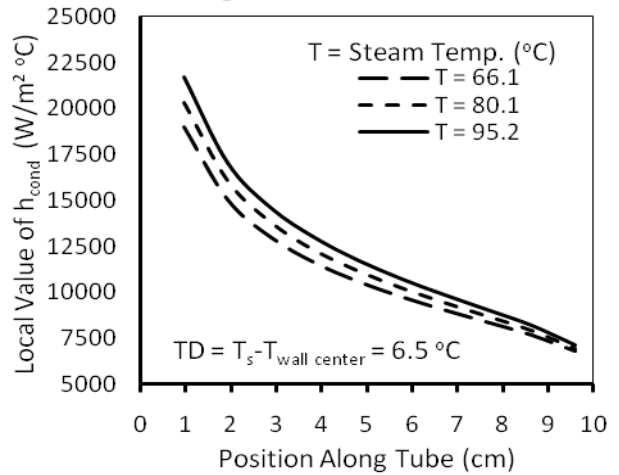


Fig. (14) Variation of local condensation H.T. coefficient with position along tube for different steam temperatures.

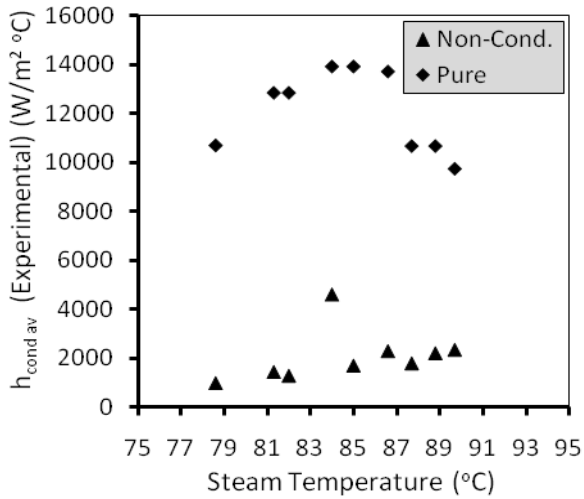


Fig. (15) Comparison of average condensation heat transfer coefficient for pure steam and with the presence of non-condensable gas (air).

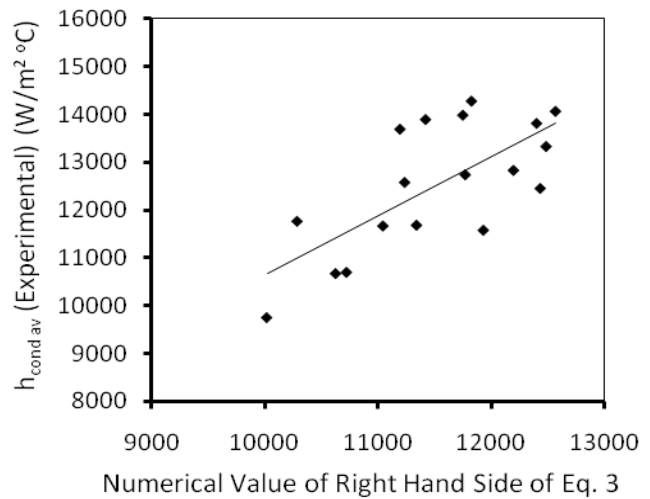


Fig. (16) Plot of experimentally calculated average condensation heat transfer coefficient versus numerical value of right hand side of Eq. 3.